Bulletin of the Seismological Society of America. Vol. 57, No. 6, pp. 1355–1365. December, 1967

EXCITATION OF MANTLE RAYLEIGH WAVES OF PERIOD 100 SECONDS AS A FUNCTION OF MAGNITUDE

By James N. Brune and Chi-Yu King*

ABSTRACT

The excitation of mantle Rayleigh waves of 100 seconds period as a function of magnitude is studied using data from 91 earthquakes in the magnitude range 5.0 to 8.9. The data were recorded on a wide variety of instruments including Milne-Shaw horizontal pendulums and modern long-period high-gain inertial seismographs. The larger earthquakes studied range in time from 1923 to 1964. Mantle Rayleigh wave amplitudes are corrected to a distance of 90° and plotted as a function of surface wave magnitude. The data are compared with theoretical curves based on a moving source model and two statistical models discussed by Aki. It is concluded that for large earthquakes the source may be approximated by a point couple which propagates a distance given approximately by the length of the aftershock zone.

Introduction

Large shallow earthquakes generate fundamental mode Rayleigh waves of periods greater than 90 seconds—herein called mantle Rayleigh waves—with sufficient amplitude to be recorded on modern long-period inertial seismographs and strain meters. It is less well-known that the largest shallow earthquakes generate mantle waves large enough to be clearly recorded on Milne-Shaw and Wiechert horizontal component mechanical pendulums which have been in operation since the early 1900's. Recently developed long-period seismographs make recording of mantle waves possible for earthquakes of magnitudes as low as 5. Unfortunately, with many older instruments being replaced by new instruments with high magnification it is now difficult to find instruments which stay on scale during very large earthquakes.

In this paper we report on a study of the excitation of mantle waves as a function of magnitude. Measurements are made on several different types of seismographs capable of recording mantle waves. The results are interpreted in terms of the expected excitation function based on Tocher's and Iida's curves for fault length versus magnitude.

Instruments

Instruments of several types were used to record the mantle waves studied in this paper. These are summarized in Table 1 which gives instrument designation and gain at a period of 100 seconds.

The Milne-Shaw horizontal mechanical pendulums have a free period of 12 seconds. The data recorded on these instruments were from Canadian stations operat-

* Now at the Institute of Geophysics and Planetary Physics, University of California, Los Angeles.

ing since 1923. The Wiechert horizontal pendulums are similar but with a free period of 8–9 seconds. Strain seismographs are those developed by Benioff (1959).

Columbia-IGY instruments are electromagnetic seismographs with pendulum period 15 seconds and galvanometer period 80 seconds. These instruments are described by Sutton and Oliver (1959). WWSSN instruments are the long-period electromagnetic seismograph of the World-Wide Standardized Seismograph Network. These instruments are described in publications of the U. S. Coast and Geodetic Survey.

The CIT ULP instruments are ultra-long period seismographs (peak response at a period of 80 seconds) with capacitor transducers and are described by Gilman (1960). The Columbia ULP filtered instruments are long-period electromagnetic seismographs using filter galvanometers to reject surface waves of periods less than 70 sec. These are described by Brune (1963).

TABLE 1

INSTRUMENTS

Earthquake No.	Stations	Instrument	Amplification at 100 sec
1–16	VIC, TNT, OTT	Milne-Shaw	4
9	PAS	Strain	30
15a	PAS	Long Period Benioff	25
16	PAS	Strain	4
17, 18, 19	RDJ, SUV	Columbia-IGY	150
	MTJ, PER, OTT, UPP	Columbia-IGY	70
18a	PAS	Strain	4.4
19a	BER, JEN	Wiechert	1.5
	KIP	Strain	28
20–25	PAL, HON	Columbia—ULP filtered	60
25	JER	WWSSN	416
	ESK	WWSSN	208
26	OGD	WWSSN	833
27	KTG, HKC	WWSSN	208
	GOL	WWSSN	416
28–33	ISA	CIT-ULP	500
34–44	PAS	CIT-ULP	500
45–88	PAS	CIT-ULP	1600

Data Analysis

A total of 91 earthquakes with magnitudes ranging from 5 to 8.9 were investigated in this study. Origin times, epicenters, depths, magnitudes, recording stations and approximate epicentral distances are listed in Table 2. The magnitude used in this study is M_s as defined by Gutenberg (1945) and is primarily based on the amplitudes of 20 second surface waves; however, it may be determined from body waves also (Gutenberg and Richter, 1956; Richter, 1958). Most magnitudes less than 7.5 were determined at Pasadena. Magnitudes greater than 7.5 were deter-

TABLE 2

Earthquake No.	Date	Origin Time h	m	s	Lat.	Long.	Depth (km)	Magnitude	Station	Epicentral Distance (degrees)	Signal Used	Log A_{90}*
1	Feb. 3, 1923	16	01	41	54 N	161 E		8.4	VIC	46	R_2	3.37†
2	June 26, 1924	01	37	34	56 S	$157\frac{1}{2}$ E		8.3	VIC	120		
											R_2	3.01†
											R_3	3.50†
3	June 17, 1928	03	19	27	$16\frac{1}{2}$ N	98 W		7.9	VIC	38	R_2	3.62†
4	June 27, 1929	12	47	05	54 S	$29\frac{1}{2}$ W		8.3	VIC	132	R_2	2.79†
5	Jan. 15, 1931	01	50	41	$39\frac{1}{2}$ S	177 E		7.9	VIC	104	R_2	2.43†
6	May 14, 1932	13	11	00	$\frac{1}{2}$ N	126 E		8.3	VIC	102	R_2	3.01†
7	June 3, 1932	10	36	50	$19\frac{1}{2}$ N	$104\frac{1}{2}$ W		8.1	TNT	32	R_2	2.66†
									VIC	32	R_2	3.27†
8	June 18, 1932	10	12	10	$19\frac{1}{2}$ N	$103\frac{1}{2}$ W		7.9	TNT	32	R_2	2.36†
									VIC	32	R_2	2.23†
9	March 2, 1933	17	30	54	$39\frac{1}{4}$ N	$144\frac{1}{2}$ E		8.9	VIC	61	R_2	3.10†
									PAS	75	R_2	3.53‡
10	Jan. 15, 1934	08	43	18	$26\frac{1}{2}$ N	$86\frac{1}{2}$ E		8.4	VIC	100	R_2	2.77†
11	July 18, 1934	19	40	15	$11\frac{3}{4}$ S	$166\frac{1}{2}$ E		8.1	TNT	118	R_2	2.60†
12	Sept. 20, 1935	01	46	33	$11\frac{3}{4}$ S	$166\frac{1}{2}$ E		7.9	TNT	118	R_1	3.05†
									VIC	86	R_1	2.73†
13	Dec. 28, 1935	02	35	22	0	$98\frac{1}{4}$ E		8.1	TNT	137	R_2	2.45†
14	Nov. 25, 1941	18	03	55	$37\frac{1}{2}$ N	$18\frac{1}{2}$ W		8.4	TNT	44	R_2	2.93†
15	Nov. 10, 1942	11	41	27	$49\frac{1}{2}$ S	32 E		8.3	VIC	160	R_3	3.44†
15a	Aug. 15, 1950	14	09	30	28.6 N	96.5 E		8.6	PAS	110	R_2	3.40‡
16	Nov. 4, 1952	16	58	26	$52\frac{3}{4}$ N	$159\frac{1}{2}$ E		8.4	OTT	73	R_3	3.55†
									PAS	59	R_2	3.74‡
17	July 10, 1958	06	15	54	$58\frac{1}{2}$ N	136 W		$7\frac{3}{4}$–8	RDJ	110	R_2	2.24‡
									PER	125	R_1	2.32
									OTT	37.8	R_2	2.64
									UPP	59.7	R_2	2.55
18	Sept. 4, 1958	21	51	08	$33\frac{1}{2}$ S	$69\frac{1}{2}$ W		$6\frac{3}{4}$–7	MTJ	150	R_1	1.41
18a	May 22, 1960	19	11	20	38 S	$73\frac{1}{2}$ W		8.4	PAS	82	R_2	3.42†
19	Aug. 9, 1960	07	39	23	40 N	126.6 W	25	6	SUV	76	R_1	1.06
19a	March 28, 1964	03	37	14.2	61.1 N	147.7 W	33	8.4	JEN		R_2	4.00
									BER		R_2	
									KIP		R_2	2.96‡
											R_3	3.42‡
20	Nov. 19, 1964	23	35	06	6.0 S	150.8 E	3	$6\frac{3}{4}$	PAL	127.1	R_1	1.50
											R_2	1.44
21	Jan. 24, 1965	00	11	12	2.4 S	126.0 E	6	$7\frac{1}{2}$–$7\frac{3}{4}$	PAL	137.6	R_1	2.66
											R_2	2.81
											R_3	2.93
									HON	77.8	R_2	3.10
22	Feb. 4, 1965	05	01	22	51.3 N	178.6 E	40	$7\frac{3}{4}$	HON	35.0	R_3	2.76
23	March 21, 1965	11	08	16	1.5 S	126.5 E	33	$6\frac{3}{4}$	PAL	136.6	R_1	1.35
24	March 28, 1965	16	33	15	32.4 S	71.2 W	72	7–$7\frac{1}{4}$	PAL	73.1	R_1	1.67
									HON	98.6	R_2	2.15
25	March 30, 1965	02	27	07	50.6 N	177.9 E	51	7–$7\frac{1}{4}$	PAL	69.3	R_2	2.41
									HON	34.8	R_1	2.01
									JER	90	R_3	2.43
									ESK	72	R_3	2.65
26	May 20, 1965	00	40	11	14.7 S	167.4 E	16	$6\frac{3}{4}$–7	OGD	120	R_3	2.03
27	Aug. 2, 1965	13	19	55	56.2 S	158.2 E	33	7–$7\frac{1}{4}$	KTG	158	R_2	1.89
									HKC	81	R_2	2.14
											R_3	2.31
									GOL	98	R_3	1.94
28	Aug. 23, 1965	19	46	02	16.3 N	95.8 W	20	$7\frac{1}{4}$	ISA	27.9	R_2	1.63
											R_3	1.87
29	Sept. 4, 1965	14	32	47	58.2 N	152.7 W	10	$6\frac{3}{4}$–7	ISA	31.9	R_1	1.37

* A = Vertical ground amplitude in microns for Rayleigh waves with periods of approximately 100 seconds.
† Value of A computed from horizontal trace amplitudes assuming $A_Z / A_H = 1.3$.
‡ Value of A computed from strain seismograph.

TABLE 2—*Continued*

Earthquake No.	Date	Origin Time			Lat.	Long.	Depth (km)	Magnitude	Station	Epicentral Distance (degrees)	Signal Used	Log A_{90}*
		h	m	s								
30	Sept. 12, 1965	08	40	11	6.4 S	151.6 E	29	6½–6¾	ISA	93.6	R_1	0.13
31	Sept. 17, 1965	11	13	56	1.5 S	77.7 W	191	6½	ISA	53.0	R_1	0.59
32	Sept. 17, 1965	16	21	19	36.3 N	141.3 E	40	6¾	ISA	77.0	R_1	1.02
33	Sept. 21, 1965	01	38	31	29.0 N	128.1 E	199	6¾	ISA	90.2	R_1	1.19
34	Sept. 30, 1965	23	47	40	59.7 N	143.4 W	12	5.3	PAS	30.5	R_1	0.46
35	Oct. 1, 1965	08	52	06	50.1 N	178.3 E	32	6½	PAS	48.3	R_1	0.55
36	Oct. 3, 1965	14	45	27	49.5 N	156.5E	33 R	6	PAS	62.1	R_1	0.01
37	Oct. 3, 1965	16	14	55	42.9 S	75.4 W	28	6½	PAS	86.1	R_1	0.77
38	Oct. 12, 1965	13	40	56	56.3 N	153.7 W	11	5.2	PAS	32.8	R_1	−0.17
39	Oct. 18, 1965	21	50	05	1.1 S	127.9 E	33 R	6¾	PAS	110.3	R_1	0.95
											R_2	1.12
40	Oct. 19, 1965	20	48	47	52.3 N	174.3 E	48 R	5.5	PAS	50.5	R_1	−0.05
41	Nov. 6, 1965	09	21	49	22.1 S	113.8 W	33 R	6	PAS	56.1	R_1	0.39
42	Nov. 12, 1965	17	52	24	30.5 N	140.2 E	40	6¾	PAS	82.1	R_1	0.64
											R_2	0.75
43	Nov. 13, 1965	04	33	53	43.8 N	87.8 E	59 R	6¾	PAS	98.9	R_1	0.76
44	Nov. 15, 1965	11	18	50	0.3 S	18.7 W	24 R	6½	PAS	97.7	R_1	1.41
											R_2	1.18
45	Nov. 16, 1965	15	24	43	31.0 N	41.5 W	17 R	6½	PAS	63.2	R_1	0.67
											R_2	0.96
46	Nov. 19, 1965	07	14	13	45.3 N	150.9 E	13	5.5	PAS	67.3	R_1	0.05
47	Nov. 21, 1965	10	31	50	6.1 S	130.4 E	93	6	PAS	111.1	R_1	0.94
											R_2	0.87
48	Dec. 6, 1965	11	34	54	18.9 N	107.1 W	37	6¾	PAS	18.1	R_2	1.26
											R_3	1.07
49	Dec. 6, 1965	18	42	33	18.8 N	107.0 W	40	5¾	PAS	18.2	R_1	−0.37
50	Dec. 22, 1965	19	41	23	58.4 N	153.0 W	50R	6¾–7	PAS	33.5	R_1	0.07
51	Jan. 15, 1966	11	59	59	59.5 N	144.6 W	33	5.0	PAS	30.7	R_1	−0.90
52	Jan. 20	04	27	45	15.1 S	168.0 E	28	5.5	PAS	88.5	R_1	−0.48
53	Jan. 22	14	27	08	56.0 N	153.7 W	33 R	6	PAS	32.7	R_1	−0.23
54	Feb. 4	10	39	12	15.9 S	167.9 E	190	5.6	PAS	86.1	R_1	0.29
											R_2	0.38
55	Feb. 5	02	01	48	39.2 N	22.0 E	38	6¼	PAS	98.2	R_1	0.42
56	Feb. 5	15	12	29	26.1 N	103.1 E	15	5.7	PAS	108.4	R_1	0.36
57	Feb. 9	04	40	28	56.7 S	25.7 W	27	5½	PAS	119.1	R_1	0.52
											R_2	0.77
											R_3	0.45
58	Feb. 10	14	21	11	20.8 N	146.3 E	43	6½	PAS	83.0	R_1	0.39
59	Feb. 16	03	18	27	17.7 S	167.9 E	31	6½	PAS	87.1	R_1	0.31
											R_2	0.37
60	Feb. 22, 1966	05	02	37	5.4 S	151.5 E	28R	6¾	PAS	93.3	R_1	0.37
61	March 6	18	01	50	24.1 S	176.9 W	33R	5.1	PAS	80.4	R_1	−0.61
62	March 11	07	54	17	55.2 S	126.6 W	33R	5.0	PAS	89.3	R_1	−1.03
63	March 12	16	31	22	24.1 N	122.6 E	63	7½–7¾	PAS	98.2	R_2	1.80
											R_3	1.91
64	March 13	17	58	36	55.0 S	126.4 W	33R	5.2	PAS	89.1	R_1	−0.66
65	March 20	01	42	50	0.6 N	30.2 E	36R	6¾–7	PAS	134.5	R_1	1.42
66	March 22	08	19	34	37.5 N	115.1 E	33	6¾–7	PAS	93.2	R_1	0.86
											R_2	0.60
67	April 6	02	59	02	45.8 S	96.1E	33	6	PAS	151.5	R_1	0.46
											R_2	0.20
68	April 10	16	36	15	31.5 S	71.2 W	64R	6	PAS	78.9	R_1	−0.34
69	April 16	01	27	15	57.0 N	153.6 W	33R	6¼	PAS	33.1	R_1	0.03
70	April 20	06	00	39	18.9 N	146.8 E	33R	5.0	PAS	83.6	R_1	−0.31
71	April 22	23	27	21	57.5 N	152.1 W	22	5.3	PAS	32.7	R_1	−0.41
72	April 23	00	09	34	0.9 S	122.4 E	45	6¾	PAS	113.5	R_1	1.27
											R_2	1.16
											R_3	1.28
73	April 23	08	56	46	0.5 S	122.2 E	79	6	PAS	113.9	R_1	0.10
											R_2	−0.04

TABLE 2—*Continued*

Earthquake No.	Date	Origin Time h	m	s	Lat.	Long.	Depth (km)	Magn-tude	Station	Epi-central Distance (degrees)	Signal Used	Log A_{90}*
74	May 1, 1966	16	22	56	8.5 S	74.3 W	165R	$6\frac{3}{4}$	PAS	59.4	R_1	0.60
											R_2	0.65
75	May 15	14	46	07	51.5 N	178.4 W	31R	$5\frac{3}{4}$–6	PAS	46.1	R_1	0.05
76	May 19	07	06	27	54.1 N	164.1 W	28	6	PAS	37.7	R_1	0.25
77	May 20	09	14	49	13.9 N	146.1 E	66	$6\frac{1}{4}$–$6\frac{1}{2}$	PAS	87.0	R_1	−0.12
78	June 1	11	47	33	23.4 S	174.9 W	24	5.0	PAS	78.6	R_1	−0.37
79	June 2	03	27	53	51.1 N	176.0 E	41R	6	PAS	49.6	R_1	−0.43
80	June 4	23	48	18	46.5 N	152.5 E	27R	$5\frac{3}{4}$–6	PAS	65.8	R_1	0.00
81	June 6	07	46	16	36.3 N	71.2 E	225R	$6\frac{3}{4}$	PAS	109.4	R_1	1.25
											R_2	1.34
											R_3	1.36
82	June 15	00	59	46	10.4 S	160.8 E	31	$7\frac{1}{2}$	PAS	88.5	R_1	1.81
											R_2	2.13
											R_3	1.57
83	June 15	01	32	56	10.2 S	161.1 E	33R	$7\frac{1}{4}$	PAS	88.1	R_1	1.58
											R_2	1.64
											R_3	1.54
84	July 4, 1966	18	33	36	51.7 N	179.9 E	13	$6\frac{3}{4}$–7	PAS	47.1	R_1	1.49
											R_2	1.66
											R_3	1.60
85	July 19	01	40	54	56.2 N	164.9 E	18	6–$6\frac{1}{4}$	PAS	55.4	R_1	0.73
86	Aug. 1	21	03	00	30.0 N	68.7 E	33R	$6\frac{3}{4}$	PAS	115.9	R_1	1.65
											R_2	1.20
87	Aug. 7	02	13	05	50.6 N	171.3 W	39R	$6\frac{3}{4}$	PAS	41.6	R_1	0.74
88	Aug. 19	12	22	10	39.2 N	41.7 E	26R	7	PAS	104.7	R_1	1.84

mined in some cases at Pasadena and in other cases both at Pasadena and Berkeley. For earlier earthquakes recorded on Milne-Shaw instruments, the magnitudes are taken from Richter (1958).

The basic data obtained are mantle Rayleigh wave ground amplitudes (vertical component) at a period of 100 seconds corrected to an epicentral distance of 90°. Amplitudes were read directly from the records and corrected for instrument response and distance effects. See Figure 1 for an example of a measurement of amplitude. Observations on horizontal component instruments were corrected for azimuth and multiplied by $\frac{4}{3}$ to convert to equivalent vertical amplitudes. For magnitudes less than 6 the data are biased toward higher amplitudes since the amplitudes for some smaller events may be too small to be recorded at large distances. However, all earthquakes with $M \geqq 6$ which occurred during the period represented by the data for the CIT ULP instrument with a gain of 1600, generated mantle waves which were recorded and included in the data. Thus there is no reason to expect bias for $M \geqq 6$.

The distance correction consists of two factors. The first factor consists of the following: (1) A correction for dispersion. This is based on theoretical seismograms corresponding to the known group velocity curve for mantle waves. This correction is proportional to the square root of distance for distances larger than about 160°. (2) A correction for geometric spreading on a sphere. This is proportional to the square root of the sine of the distance in degrees, except near the epicenter and antipodes. Near the epicenter and antipodes it is proportional to $\sqrt{\pi n/2}/P_n\ (\cos \Delta)$, where $P_n\ (\cos \Delta)$ is the Legendre polynomial of order n, and $n + \frac{1}{2}$ is equal to the radius of the earth divided by the wavelength. However, measurement of amplitude within a wavelength of the epicenter or antipodes will probably not be reliable since waves arriving from many directions interfere. (3) A correction for attenuation. This is given by exp $(\pi x/QUT)$ where Q is taken as 145 (Ben-Menahem, 1965), x is the distance, U the group velocity, and T the period (100 seconds).

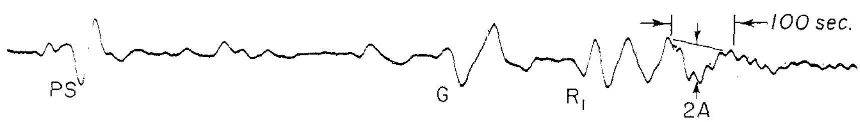

FIG. 1. Seismogram illustrating mantle Rayleigh wave train R_1 and method of measuring amplitude. This seismogram is for the Tonga Island earthquake of 21 December 1959 ($M = 6$) recorded on a CIT ULP instrument at Pasadena (Gilman, 1960).

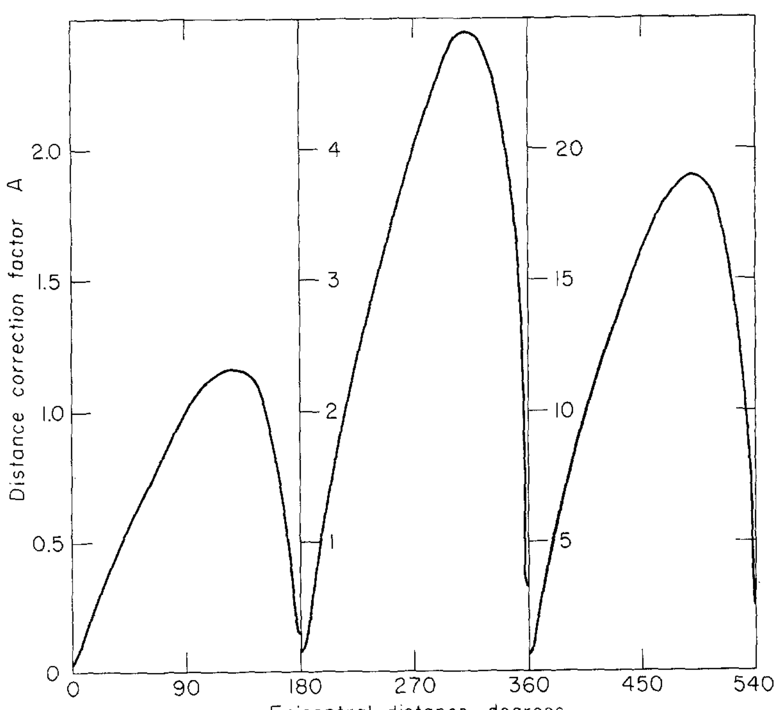

FIG. 2a. Distance correction factor, A, for 100 second period mantle Rayleigh waves.

The product of these corrections, A, is given as a function of distance in Figure 2a.

A further empirical correction factor was determined by numerous correlations of R_1 to R_3 and R_1 to R_2. This empirical factor corrects for effects such as:

(1) Change in the shape of the spectrum as a function of distance. This will change the ratio of the observed trace amplitude to the true spectral amplitude.

(2) Uncertainty in the appropriate Q value and deviations from an exact exponential attenuation.

(3) Abnormal dispersion, due in part to scattering and refraction.

(4) The effect of the shape of the response curve for a particular type of instrument. This effects the distance dependence of trace amplitude at distances of the order of 100° and less. The empirical correction factor obtained here in a strict sense only applies to the CIT ULP instrument; however, the effect is small and probably nearly the same for the other instruments used in this study.

This empirical correction factor, B, is determined to be a factor of 1.6 at $\Delta = 270°$ and 2.3 at $\Delta = 450°$. It is approximated as a linear function of distance and shown in Figure 2b.

The logarithms of the ground amplitudes in microns, corrected to a distance of

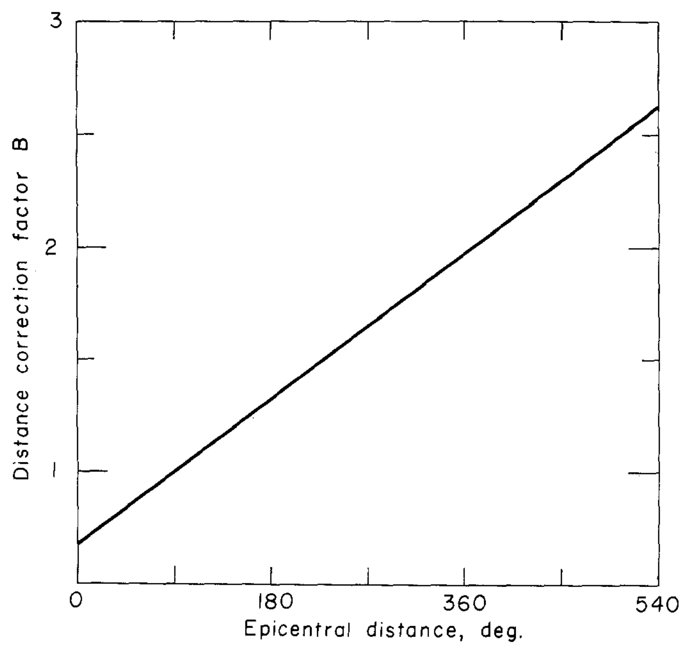

FIG. 2b. Distance correction factor, B, for 100 second period mantle Rayleigh waves.

90°, are shown in Table 2 and plotted as a function of magnitude in Figure 3. Most of the earthquakes used have depths less than 60 km, but the few deeper ones, with depths up to 225 km, give results comparable to the shallow shocks. For these deeper quakes the magnitude M was determined from body waves.

THEORETICAL CURVE

Large shallow earthquakes are often associated with long surface breaks and long aftershock zones. Tocher (1958), Iida (1959; 1965) and Albee and Smith (1966), have given curves of approximate length of faulting or length of aftershock zone versus magnitude. The propagation of the seismic source should control the ratio of the amplitudes of 100 second waves to 20 second waves and thus the excitation of mantle waves as a function of magnitude. The effect of a propagating source can be derived quite simply (Benioff, 1955; Ben-Menahem, 1961; Haskell, 1963). The effect is to multiply the amplitude spectrum by the directivity function, sin X/X, (Ben-Menahem, 1961) where:

$$X = \frac{-\pi b}{cT}\left(\frac{c}{v} - \cos\phi\right)$$

In this expression b is the fault length, c the phase velocity, T the period, v the fault propagation velocity, and ϕ the angle between the direction of fault propagation and the direction to the recording station.

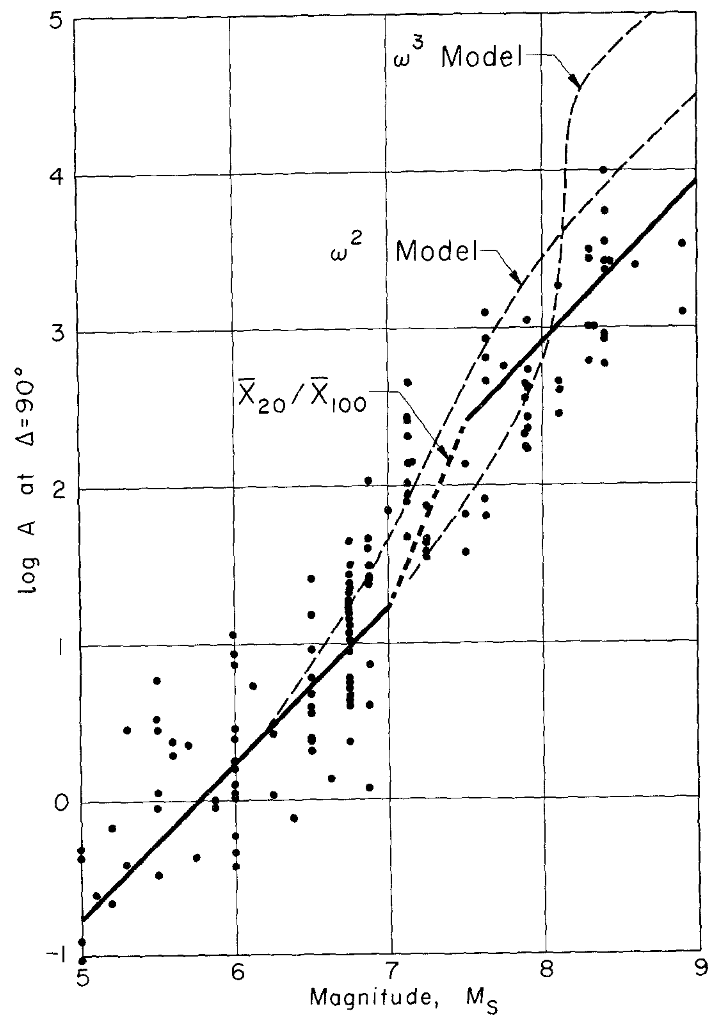

FIG. 3. Logarithm to the base 10 of the amplitude of vertical ground motion (in microns) of 100 second period mantle Rayleigh waves at a distance of 90°, plotted as a function of magnitude M_s. The curve labeled X_{20}/X_{100} is based on a traveling source model and the curves labeled ω^2 and ω^3 are based on models discussed by Aki (1967).

In order to obtain an approximate theoretical curve for the amplitudes of 100 second mantle waves as a function of magnitude, we proceed as follows:

We assume that the earthquake magnitude is directly proportional to the amplitude of 20 second surface waves as implied by the surface wave magnitude scale. We then compute the ratio of the directivity function for 100 second mantle waves to that for 20 second surface waves as a function of fault length (or length of aftershock zone), assuming further that $v = 3$ km/sec,

$$R(b) = \frac{\sin X_{100}/X_{100}}{\sin X_{20}/X_{20}}.$$

This function in general will have zeros and infinities in it due to the sine functions, but by making a large number of observations we will tend to average out these effects. We shall assume that the erratic behavior of $R(b)$ is smoothed by averaging the scatter in the observed data, so that $\overline{R(b)} \simeq \overline{X}_{20}/\overline{X}_{100}$ (= 5 for large fault lengths since the average value of cos ϕ is zero).

Having $\overline{R(b)}$ as a function of fault length and having a relationship between fault length and magnitude, we obtain a theoretical curve for excitation of mantle waves as a function of magnitude. The curve given in Figure 3 (labelled $\overline{X}_{20}/\overline{X}_{100}$) is determined from relationships between fault length and magnitude given by Tocher (1958) and Iida (1958; 1965) by smoothing into three straight line segments. The portion of the curve above magnitude 7 reflects the interference effects of the propagating rupture. The absolute value of the curve agrees at $M = 6$ with the theoretical amplitude ratio of 100 second to 20 second Rayleigh waves for a point couple in a layer over a half-space (computed from the theory of Yanovskaya, 1958, assuming a Q of 400 for 20 second Rayleigh waves).

Aki (1967) has recently used a statistical or incoherent source model proposed by Haskell (1966) to derive a scaling law for seismic spectrum. This model is referred to as the ω^3 model since it predicts the amplitude spectrum for an earthquake will decrease as $1/\omega^3$ at high frequencies. Aki proposed another model based on similar considerations but having a decrease in amplitude proportional to $1/\omega^2$ at high frequencies. This model is referred to as the ω^2 model and agrees with the data presented by Aki much better than does the ω^3 model. From curves presented by Aki we can directly obtain the 100 second to 20 second amplitude ratio as a function of magnitude for the ω^2 and ω^3 models. The corresponding curves are shown in Figure 3.

Discussion

The data shown in Figure 3 indicate a range of amplitude of somewhat greater than a factor of ten at any given magnitude. This is considerably less than the range of amplitudes of 20 second surface waves for a given local earthquake magnitude based on waves of about 1 sec period (Brune *et al*, 1963), suggesting that mantle waves are a more reliable measure of earthquake size than shorter period waves. This is not unexpected since these very long wavelengths should not be as strongly influenced by interference and local effects. A mantle wave magnitude scale based on the solid curve in Figure 3 would thus have some merit.

The data agree well with the X_{20}/X_{100} curve, indicating that on the average earthquakes can be adequately modelled by a propagating rupture, with the length of rupture approximately as given by Tocher's and Iida's curves.

The data agree better with the ω^2 than with the ω^3 model, but nevertheless lie significantly below both models for $M > 8.0$. For the ω^3 model the scale effect increases sharply at $M = 8.0$ and for $M = 8.4$ gives amplitudes of 100 sec waves

25 times greater than the average of the observed data. For the ω^2 model the scale effect increases the curve gradually from $M = 6$ and it gives amplitudes about 4 times higher than the mean of the data beyond $M = 8.0$. Thus the increase in the 100 sec to 20 sec amplitude ratio with increasing magnitude is much less than predicted by the ω^3 model and somewhat less than predicted by the ω^2 model. This may be due to the lack of strict similarity between large earthquakes and smaller ones. Tocher (1958) interpreted his data as indicating that for large earthquakes the fault length increases at a much faster rate than fault depth, thus violating the rule of similarity assumed by Aki. The data might also be explained by the type of incoherency in the source region. The data in Figure 3 indicate that the scale effect on the amplitude ratio of 100 to 20 second waves from magnitude 6 to magnitude 8.4 is about a factor of 5 in agreement with the $\overline{X}_{20}/\overline{X}_{100}$ model. A factor of 20 is predicted by the ω^2 model and a factor of 125 by the ω^3 model. This suggests that if a scaling law appropriate for this frequency and magnitude range is to be constructed it would be of the ω type, i.e., the spectral amplitudes for a given earthquake would be proportional to $1/\omega$. If we accept Aki's ω^2 model for shorter periods then the data indicate that a different type of incoherency occurs for periods of about 20 seconds. Haskell (personal communication) has pointed out that the displacement spectrum at high frequencies must fall off faster than $\omega^{-3/2}$ in order to keep the energy integral finite.

Acknowledgments

One of the authors (Chi-Yu King) was a post-doctoral fellow at the California Institute of Technology while participating in the study. Special thanks are due to Mr. Robert Eppley of the U. S. Coast and Geodetic Survey who made many of the amplitude readings from Columbia ULP records and to Mr. Ralph Gilman who provided records from the Pasadena (PAS) ULP instruments and assisted in the preparation of the paper. The authors are indebted to Professor Keiiti Aki for critically reading the manuscript and offering constructive criticism. Professor Stewart Smith provided records and calibration curves for the Isabella (ISA) station. This research was supported in part by the U. S. Coast and Geodetic Survey under contract CGS 1091 (G) while the first author was at Lamont Geological Observatory, the National Science Foundation under grant GP 2806, and the Air Force Office of Scientific Research, Office of Aerospace Research, United States Air Force, under AFOSR contract AF-49(638)-1337.

References

Aki, K. (1967). Scaling law of seismic spectrum, *J. Geophys. Res.* **72,** 1217–1231.

Albee, A. L. and J. L. Smith (1966). Earthquake characteristics and fault activity in southern California, engineering geology of southern California, *Assoc. Engineering Geologist,* 9–33.

Benioff, H. (1955). Mechanism and strain characteristics of the White Wolf fault as indicated by the aftershock sequence, *Calif. Div. Mines, Bull.* 171, 199–202.

Benioff, H. (1959). Fused-quartz extensometer for secular, tidal and seismic strains, *Bull. Geol. Soc. Am.* **70,** 1019–1032.

Ben-Menahem, A. (1961). Radiation of seismic surface-waves from finite moving sources, *Bull. Seism. Soc. Am.* **51,** 401–435.

Ben-Menahem, A. (1965). Observed attenuation and Q values of seismic surface waves in the upper mantle, *J. Geophys. Res.* **70,** 4641–4651.

Brune, J. N. (1963). Use of surface wave rejection filters to record mantle waves of lower order, *Earthquake Notes,* **34,** 73.

Brune, J. N., A. Espinosa and J. E. Oliver (1963). Relative excitation of surface waves by earthquakes and underground explosions in the California-Nevada region, *J. Geophys. Res.* **68,** 3501–3513.

Gilman, R. (1960). Report on some experimental long-period seismographs, *Bull. Seism. Soc. Am.* **50**, 553–559.

Gutenberg, B. (1945). Amplitudes of surface waves and magnitudes of shallow earthquakes, *Bull. Seism. Soc. Am.* **35**, 3–12.

Gutenberg, B., and C. F. Richter (1956). Magnitude and energy of earthquakes, *Ann. Geofis.* **9**, 1–15.

Haskell, N. A. (1963). Radiation pattern of Rayleigh waves from a fault of arbitrary dip and direction of motion in a homogeneous medium, *Bull. Seism. Soc. Am.* **53**, 619–642.

Haskell, N. A. (1964). Total energy and energy spectral density of elastic wave radiation from propagating faults, *Bull. Seism. Soc. Am.* **54**, 1811–1841.

Haskell, N. A. (1966). Total energy and energy spectral density of elastic wave radiation from propagating faults, Part II. A statistical source model, *Bull. Seism. Soc. Am.* **56**, 125–140.

Iida, K. (1959). Earthquake energy and earthquake fault, *J. Earth Sci., Nagoya Univ.* **7**, 98–107.

Iida, K. (1965). Earthquake magnitude, earthquake fault, and source dimension, *J. Earth. Sci., Nagoya Univ.* **13**, 115–132.

Richter, C. F. (1958). *Elementary Seismology*, W. H. Freeman and Co., San Francisco.

Sutton, G. and J. Oliver (1959). Seismographs of high amplification at long periods, *Annales Geophys.* **15**, 423.

Tocher, D. (1958). Earthquake energy and ground breakage, *Bull. Seism. Soc. Am.* **48**, 147–153.

Wyss, M. and J. N. Brune (1967). The Alaska earthquake of 28 March 1964: A complex multiple rupture, *Bull. Seism. Soc. Am.* **57**, 1017–1023.

Yanovskaya, T. B. (1958). On the determination of the dynamic parameters of the focus hypocenter of an earthquake from records of surface waves, *Bull. (Izvestiya), Acad. of Sciences, U.S.S.R., Geophys. Series, No. 3*, 289–301.

SEISMOLOGICAL LABORATORY
CALIFORNIA INSTITUTE OF TECHNOLOGY
PASADENA, CALIFORNIA
DIVISION OF GEOLOGICAL SCIENCES CONTRIBUTION NO. 1462.

LAMONT GEOLOGICAL OBSERVATORY
COLUMBIA UNIVERSITY
PALISADES, NEW YORK
CONTRIBUTION NO. 1126

Manuscript received May 16, 1967.